

Interaction of high order solitons with external dispersive waves

I. Oreshnikov¹ and R. Driben^{2,3}

¹*Department of Physics, St. Petersburg State University, 198504, Ulyanovskaya st. 1, Peterhof, St. Petersburg, Russian Federation*

²*ITMO University 197101, Kronverksky pr. 49, St. Petersburg, Russian Federation*

³*Department of Physics and CeOPP, University of Paderborn, Warburger Str. 100, D-33098 Paderborn, Germany*

(Dated: October 1, 2018)

We have presented theoretical and numerical studies on interactions of dispersive waves with second order solitons. Dispersive wave with considerable intensity resonantly colliding with the second order solitons can lead to acceleration/deceleration of the later with subsequent central frequency shifts, but still well preserve the oscillating structure of the 2-solitons. The 2-soliton creates an effective periodical refractive index profile and thus reflected and transmitted dispersive waves generate new spectral bands with sharp peak structures. When resonant dispersive waves interact with two second order solitons bounding them, multiple scattering with multiple frequency conversion of the radiation occurs. Thus 2-solitons and radiation trapped in between them can produce effective solitonic cavity with "flat" or "concave mirrors" depending on the intensity of the input.

Optical solitons attract attention of researches for decades due to the profound interest of their fundamental physics and technological applications [1]. In addition to the fundamental solitons, integrable models and physical media described by nearly-integrable equations [2] support high order N -solitons, with $N \geq 2$, which are oscillating pulses periodically restoring their shape at distances that are multiples of the fundamental soliton period [3]. Experimental realization of 2- and 3-order optical solitons dates back to 1983 [4]. Initial narrowing of higher-order solitons was observed for soliton's orders up to 13 [5]. Higher-order solitons were also demonstrated in the cavity of a mode-locked dye laser [6]. Strongly oscillating higher-order solitons find natural applications for the pulse compression [7, 8] and frequency conversion [9], while the breakup of high order solitons initiates the extremely important process of the supercontinuum generation [10].

Propagation of optical pulse close to zero dispersion wavelength makes important consideration of high order dispersion terms and in particular the third order dispersion (TOD) term. Second order solitons (2-solitons) were found to be practically robust under the influence of moderate TOD [11], preserving their periodically oscillating nature. Very recently resonant radiation of 2-solitons was investigated [14] revealing fascinating structure of radiation band consisting of multiple frequency peaks. While emitting the mentioned above radiation 2-soliton remained its fundamental features for many periods. Interestingly, oscillating dissipative solitons featuring similar radiation behavior were reported too [12, 13].

It is relevant to mention that extensive studies were performed considering scattering of weak DWs on fundamental solitons, with solitons properties remaining invariant [15–20]. On the other hand, it was also demonstrated that strong resonant collision of DWs with soli-

tons can accelerate or decelerate solitons. These accelerations manifest themselves in frequency domain by upshifts or downshifts of central frequencies of the solitons [21–24]. Generation of new bands of frequencies due to the scattering of DWs from solitons can be viewed as an alternative technique for generation of broad and coherent supercontinuum [23] without the high order soliton fission.

Taking one step further a very interesting scenario with DWs interacting with two co-propagating solitons [25–27]. DWs temporally located in between the solitons interact with one soliton after the other bouncing of them. This process can repeat itself many times resulting in creation of solitonic cavity behaving like two mirrors for the DWs. In case of DWs with considerable intensity, the two solitons get attracted one towards the other, resulting in collision or even fusion [28]. This phenomenon was proven to be responsible for the appearance of multiple soliton knot patterns [21, 26, 29] during the complex supercontinuum generation process. Such a solitonic cavity was very recently successfully realized in experimental conditions [27]. Also a "convex mirror" cavity with mutually repulsing via DW two dark solitons was demonstrated [30].

In the present work we aim to study interactions of 2-solitons with external dispersive waves (DWs), demonstrating a possibility to manipulate propagation trajectories of the 2-solitons, to create broad continuum with rich spectral properties and also to create solitonic cavities consisting of two 2-solitons and DWs bouncing between them.

Dynamics of optical pulse in the vicinity of zero dispersion wavelength (ZDW) is governed by nonlinear Schrödinger equation with the inclusion of TOD.

$$i\partial_z u - \frac{1}{2}\beta_2\partial_t^2 u - \frac{i}{6}\beta_3\partial_t^3 u + \gamma|u|^2 u = 0 \quad (1)$$

where β_2 and β_3 designate second and third order dispersion terms, while γ represents the nonlinear parameter. Considering standard fiber with $\lambda_{ZDW} = 1311$ nm and launching a soliton at central wavelength of $\lambda_{sol} = 1470$ nm, we will work with the following values of dispersion parameters: $\beta_2 = -14.2$ ps²/km and $\beta_3 = 0.087$ ps³/km. The nonlinear coefficient is taken $\gamma = 2$ W⁻¹km⁻¹.

The injected light consist of two pulses launched with different frequencies namely soliton and DW

$$u_0(t) = u_{sol}(t) + u_{DW}(t)$$

The 2-soliton has the initial form

$$u_{sol}(t) = 2\sqrt{P_0} \operatorname{sech}(t/T_0)$$

with temporal width of $T_0 = 62.5$ fs and the peak power of corresponding fundamental soliton $P_0 = 1817$ W. DW is given by

$$u_{DW}(t) = A_{DW} \operatorname{sech}((t - t_1)/T_1) \exp(-i\delta\omega(t - t_1))$$

Here A_{DW} represent the amplitude of DW, t_1 the temporal delay of the DW with the respect to the soliton, T_1 is the temporal width of dispersive wave, and $\delta\omega$ is the angular frequency deviation of the DW from the soliton given by $\delta\omega = 2\pi c(\lambda_{inc}^{-1} - \lambda_{sol}^{-1})$.

The result of collision of a relatively wide DW ($T_1 = 20T_0$) centered at 1130 nm and having a very small amplitude of $A_{DW}^2 = 4.54$ W with the 2-soliton is presented in Fig. 1(a, b). Fig. 1(a) demonstrates dynamics in temporal domain and it reveals that the DW is partially scattered and partially transmitted through the 2-soliton that creates an effective periodic refractive index potential. In general one can archive much higher percentage of scattering by optimizing the incident wavelength of the DW within the resonance band, but here we aim to inspect also the transmitted part of the DW. Looking at the spectral domain representation of the dynamics in Fig. 1(b) we can see several new frequency bands arising in a course of evolution. The leftmost band below 1100 nm consisting of multiple peaks is the resonant or Cherenkov radiation [31] emitted form the 2-soliton. Its central spectral position as well as the separation between the frequency peaks is described by [14]:

$$\frac{1}{2}\beta_2\delta\omega^2 + \frac{1}{6}\beta_3\delta\omega^3 - v_g^{-1}\delta\omega = \frac{1}{2}\gamma P + \frac{2\pi}{Z_0}N$$

Here $\delta\omega = 2\pi c(\lambda^{-1} - \lambda_{sol}^{-1})$ is frequency detuning of the resonant wave from the soliton frequency, v_g is the soliton velocity, Z_0 is a period of the oscillations of 2-soliton and N is an integer number.

The region of transmitted and reflected radiation at the output of the fiber is shown in Fig. 1(c). The resonance frequencies for the radiation generated by FWM mixing between incident DW and 2-soliton were derived

by using the perturbation theory similar to the analysis for the fundamental soliton in [16]. In contrast with the fundamental soliton case, the resonant radiation becomes polychromatic, with frequency detunings for incident and scattered fields $\delta\omega_{inc, sc} = 2\pi c(\lambda_{inc, sc}^{-1} - \lambda_{sol}^{-1})$ being tied by the following relation

$$\frac{1}{2}\beta_2\delta\omega_{sc}^2 + \frac{1}{6}\beta_3\delta\omega_{sc}^3 = \frac{1}{2}\beta_2\delta\omega_{inc}^2 + \frac{1}{6}\beta_3\delta\omega_{inc}^3 + \frac{2\pi}{Z_0}N \quad (2)$$

We solved the (2) graphically in order to obtain the spectral positions of the transmitted and reflected peaks and presented it in Fig. 1(d). For example the intersection of the blue curve with the horizontal magenta line represents the scattered and transmitted DWs of the zero order ($N = 0$), that corresponds to the strongest reflected peak at about 1223 nm and strongest transmitted peak at 1130 nm. The intersection of the blue curve with the horizontal green line stand for $N = -1$ and so on. Comparison between these results and those obtained by direct numerical simulations (Fig. 1(c)) is visualized by vertical dashed lines. We can find an excellent agreement between the two approaches with a discrepancy of only few nanometers.

Using more narrow incident DWs with the temporal width equal to that of the soliton ($T_1 = T_0$) we have produced systematic simulations to provide the dependence of the scattered radiation central wavelength vs. the incident central wavelength as shown in Fig. 2. Solid curve is the plot of the analytical relation $\lambda_{sc}(\lambda_{inc})$ that is obtained from graphical solution of (2) for the fundamental harmonic $N = 0$. Shifting t_1 and thus modifying the place of collision with the respect to soliton's shape at the moment of the collision did not significantly influence the results.

Now we will inspect what happens when DW with more considerable intensity collides with the 2-soliton. In this case the velocity of the soliton will be modified and we can no longer rely on analytical approximations, but to study only results of numerical simulations. We collide DW with the 2-soliton as in the previous chapter, but this time we increase its input intensity to $A_{DW}^2 = 454.4$ W, that is still several times smaller that the input peak intensity of the 2-soliton participating in the collision and we will take the width of the DW equal to that of the soliton ($T_1 = T_0$). A typical result of collision of strong DW with the 2-soliton still resisting to the splitting is presented in the Fig. 3. The soliton's trajectory is considerably shifted, consequently it central wavelength is downshifted from 1470 nm to 1463 nm. We can also observe in Fig. 3 (lower panel) generation of significant new light spectral bands in region between the soliton's central wavelength and DW. Increasing the intensity of the incident DW much higher we will be observing the splitting of the 2-soliton.

Even more interesting interaction scenario occurs when DW bounces off two co-propagating 2-solitons. We con-

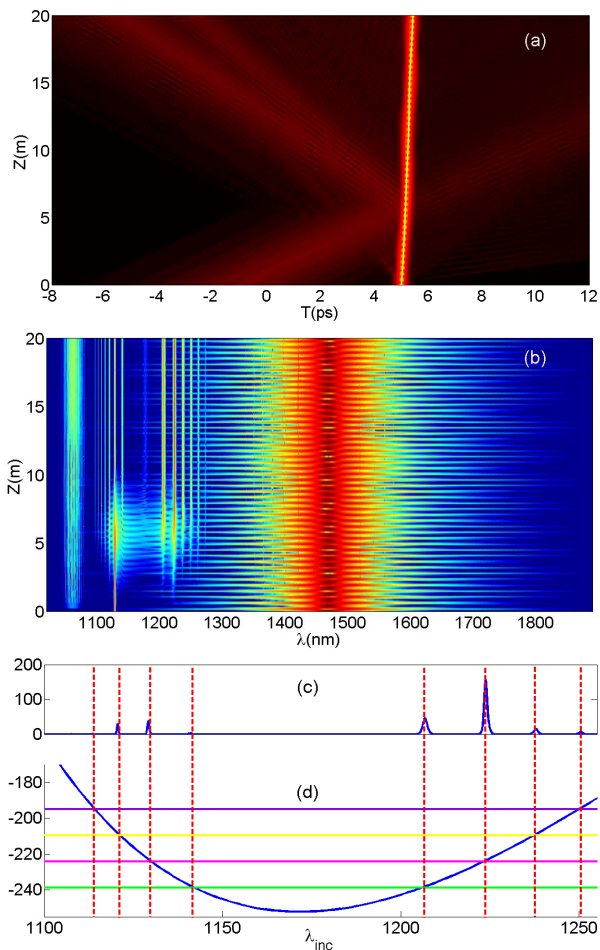


FIG. 1: (Color online) Scattering of a wide DW on 2-soliton. Dynamics in (a) temporal domain with $|u|^{0.5}$ shown instead of the conventional intensity in order to observe better less intense regions. (b) Spectral domain dynamics presented in logarithmic scale. (c) The spectral density at the end output of the fiber with the region of reflected and transmitted DW zoomed (from 1100 nm to 1255 nm). (d) is the graphical solution to (2) predicting the position of the resonance frequencies. Blue curve is the left hand side of the equation; horizontal lines correspond to the right hand's side for $N = -1, 0, \dots, 3$ starting from the bottom.

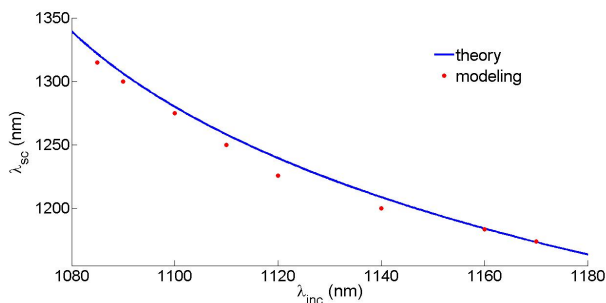


FIG. 2: (Color online) Central wavelength of the scattered radiation as a function of incident. Solid line is the curve predicted by (2) for fundamental ($N = 0$) harmonic. Square markers are found by numerical modeling.

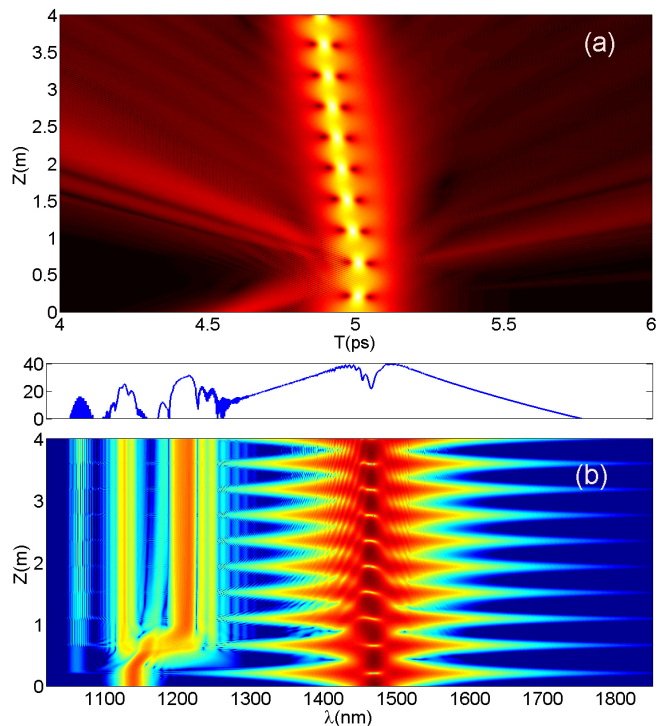


FIG. 3: (Color online) Interaction of a strong DW with 2-soliton. Dynamics in (a) temporal domain showing $|u|^{0.5}$. (b) Spectral domain dynamics representation in logarithmic scale.

sider an input consisting of two well separated 2-solitons and DW launched in between them such as

$$u_0(t) = 2\sqrt{P_0} \operatorname{sech}((t + t_1)/T_0) + A_{DW} \operatorname{sech}(t/T_0) \exp(-i\delta\omega t) + 2\sqrt{P_0} \operatorname{sech}((t - t_1)/T_0)$$

If the wavelength of DW is located well inside the resonance band we will be able to observe its multiple reflections from the 2-solitons. If the intensity of the DW is not very high the trajectories and the spectral characteristics of the two solitons are almost not modified and reflections occur pretty periodically to certain wavelength regions. For example the DW initially launched at 1140 nm with $A_{DW}^2 = 18.17$ W is being reflected several times to the region around 1200 nm and then back to its original spectral location (Fig. 4(a, b)). Interestingly the spectrum of the two solitons manifests multiple periodically alternating light and dark regions spanned for this particular example from 1250 nm to 1750 nm. Such an illumination spectrum that can be further controlled by the parameters of the participating solitons can be suggested for photonics applications requiring particular spectral design.

As mentioned above 2-solitons feature high degree of robustness when colliding with DWs and thus we can build a closed cavity consisting of two 2-solitons acting like concave mirrors without observing their splitting. An

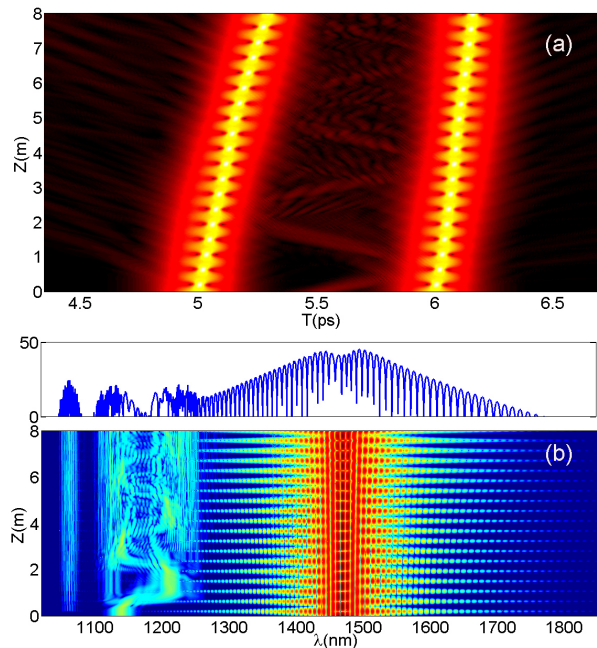


FIG. 4: (Color online) Solitonic cavity created by two 2-solitons and DW bouncing between them. (a) Temporal domain representation with $|u|^{0.5}$ shown. (b) Spectral domain representation with output spectrum profile shown above the panel.

example of such cavity is demonstrated in Fig. 5(a, b). Here we used the same type of input light but increased an intensity of the incident DW to $A_{DW}^2 = 90.85$ W leaving the rest of the parameters unchanged. In this example the central wavelength of the left and right 2-solitons get upshifted and downshifted respectively. Also the periodicity of illuminated regions such as in Fig. 4 gets strongly distorted (Fig. 5(b)).

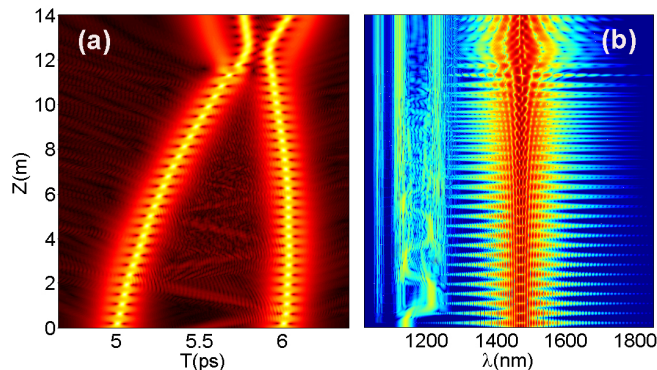


FIG. 5: (Color online) Solitonic "concave mirror" cavity created by two 2-solitons and stronger DW bouncing between them. (a) Temporal domain representation with $|u|^{0.5}$ shown. (b) Spectral domain representation.

To conclude, scattering of DWs on high order solitons was presented. The structure of the 2-soliton provides

an effective periodical potential leading to polychromatic scattering and transmission for the incident DWs. In spectral domain it manifest itself by the generation of frequency comb like novel bands. Position of the peaks of the transmitted and reflected bands is predicted by excellently overlapping analytical and numerical approaches. Interaction of DWs with two 2-solitons bounding them and creation of solitonic cavities was also demonstrated. The presented nonlinear dynamics besides the fundamental interest suggest prospective photonic devices schemes for frequency conversion and broadband light generation with pre-designed spectrum.

Funding Information

R.D. gratefully acknowledges the support by the Russian Federation Grant 074-U01 through ITMO Early Career Fellowship scheme.

-
- [1] Kivshar Y. S. and Agrawal G. P., *Optical Solitons: From Fibers to Photonic Crystals* (Academic Press, San Diego, 2003).
 - [2] Y. S. Kivshar and B. A. Malomed, *Rev. Mod. Phys.* 61, 763-915, (1989).
 - [3] J. Satsuma and N. Yajima, *Suppl. Progr. Theor. Phys.* 55, 284306 (1974).
 - [4] R. H. Stolen, L. F. Mollenauer, W. J. Tomlinson, *Opt. Lett.* 8, 186 (1983).
 - [5] L. F. Mollenauer, R. H. Stolen, J. P. Gordon, W. J. Tomlinson, *Opt. Lett.* 8, 289 (1983).
 - [6] F. Salin, P. Grangier, G. Roger, A. Brun, *Phys. Rev. Lett.* 56, 1132 (1986).
 - [7] K. C. Chan and M. S. F. Liu, *IEEE J. Quantum Electron.* 31, 2226-2235 (1995)
 - [8] Qian Li, J.N. Kutz, P.K.A. Wai, *J. Opt. Soc. Am. B*, 27 21802189 (2010)
 - [9] K. S. Lee, J. A. Buck, *J. Opt. Soc. Amer. B, Opt. Phys.* 20, 514-519 (2003)
 - [10] J. M. Dudley, G. Genty, and S. Coen, *Rev. Mod. Phys.* 78, 1135-1184 (2006).
 - [11] P. K. A. Wai, C. R. Menyuk, Y. C. Lee, and H. H. Chen, *Opt. Lett.* 11, 464-466 (1986).
 - [12] A. Bendahmane, F. Braud., M. Conforti, B. Barviau, A. Mussot, and A. Kudlinski, *Optica* 1, 243-249, (2014).
 - [13] M. Conforti, S. Trillo, A. Mussot, and A. Kudlinski, *Sci. Rep.* 5 9433 (2015).
 - [14] R. Driben, A.V. Yulin, and A. Efimov, *Opt. Express* 23 (15), 19112-19117 (2015).
 - [15] A.V. Yulin, D.V. Skryabin and P. St. J. Russell, *Optics Lett.* 29, 2411-2413, (2004).
 - [16] D.V. Skryabin and A.V. Yulin, *Phys. Rev. E* 72, 016619 (2005).
 - [17] A. Efimov, A. V. Yulin, D. V. Skryabin, J. C. Knight, N. Joly, F. G. Omenetto, A. J. Taylor, and P. Russell, *Phys. Rev. Lett.* 95, 213902 (2005)
 - [18] A. Efimov, A. J. Taylor, A. V. Yulin, D. V. Skryabin, and J. C. Knight, *Opt. Lett.* 31(11), 16241626 (2006).

- [19] D. V. Skryabin and A. V. Gorbach, *Rev. Mod. Phys.* 82, 12871299 (2010).
- [20] A Bendahmane, A Mussot, M Conforti, A Kudlinski, *Optics Express* 23, 16595 (2015)
- [21] R. Driben, F. Mitschke, and N. Zhavoronkov *Optics Express*, 18, 25993 (2010).
- [22] A. Demircan, Sh. Amiranashvili, and G. Steinmeyer, *Phys. Rev. Lett.* 106, 163901 (2011).
- [23] A. Demircan, S. Amiranashvili, C. Bre, and G. Steinmeyer, *Phys. Rev. Lett.* 110(23), 233901 (2013).
- [24] L. Tartara *JOSA B* 32, 395 (2015).
- [25] A. V. Yulin, R. Driben, B. A. Malomed, and D. V. Skryabin, *Opt. Exp.* 21, 14481-14486 (2013).
- [26] R. Driben, A.V. Yulin, A. Efimov and B.A Malomed, *Opt. Express* 21 (16), 1909119096 (2013).
- [27] S. F. Wang, A. Mussot, M. Conforti, X. L. Zeng, and A. Kudlinski, *Optics Letters* 40, 3320 (2015).
- [28] R. Driben and I.V. Babushkin, *Optics Letters* 37, 24, 51575159 (2012).
- [29] R. Driben, B. A. Malomed, A.V.Yulin, and D.V. Skryabin, *Physical Review A* 87, 063808 (2013).
- [30] I. Oreshnikov, R. Driben, and A.V.Yulin, <http://arxiv.org/abs/1508.05596>.
- [31] N. Akhmediev and M. Karlsson, *Phys. Rev. A* 51, 2602 (1995).